Title

DOPPLER LINE SHAPE OF ATOMIC FLUORESCENCE EXCITED BY MOLECULAR PHTOTDISSOCIATION

Authors

Zare, Richard N.
Herschbach, Dudley R.

Publication Date

1962-08-01

UCRL-10411

University of California

Ernest O. Lawrence Radiation Laboratory

Berkeley, California

DISCLAIMER

Submitted for publication in Proceedings
Inst. of Radio Engineers

UCRL-10411

UNIVERSITY OF CALIFORNIA

Lawrence Radiation Laboratory
Berkeley, California

Contract No. W-7405-eng-48

DOPPLER LINE SHAPE OF ATOMIC FLUORESCENCE EXCITED BY MOLECULAR PHOTODISSOCIATION

Richard N. Zare and Dudley R. Herschbach

August 1962

DOPPLER LINE SHAPE OF ATOMIC FLUORESCENCE EXCITED BY MOLECULAR PHOTODISSOCIATION*

Richard N. Zare and Dudley R. Herschbach
Department of Chemistry and Lawrence Radiation Laboratory
University of California, Berkeley, California

Abstract

A semiclassical treatment of the photodissociation of a diatomic molecule is developed. It is shown that the angular distribution of products will often be peaked parallel or perpendicular to the direction of the incident light beam. The form of the anisotropy is usually determined just by the orientation of the electronic transition dipole moment within the molecule and the polarization of the exciting light. From the angular distribution, the Doppler line shape of fluorescence emitted by an excited fragment atom is derived by averaging the geometrical factors over the translational velocity distribution of the parent molecules and the distributions in magnitude and angle of the recoil velocity of the excited atoms. A comparison is made with dissociative electron impact processes which show similar features. The photodissociation of NaI is treated in detail, and the factors influencing the fluorescence width are evaluated for possible optical maser systems in which the supply of excited atoms is generated by molecular dissociation.

---

*Received by the IRE, August, 1962. Support of this research by the Atomic Energy Commission and the Alfred P. Sloan Foundation is gratefully acknowledged.

In optical masers having a gas as the active medium the pumping mechanisms tried thus far have utilized transitions between atomic energy levels.[1-3] Many molecular dissociative processes which produce excited atoms are known, however.[4] As pointed out by Singer and Gorog,[5-7] these processes offer attractive possibilities for maser systems, since the pumping is irreversible, may be relatively broadband, and can continuously generate an almost completely inverted population of excited atoms. The conditions required to obtain coherent amplification or oscillation by stimulated emission of the atomic fluorescence line may be determined from the fundamental analysis of Schawlow and Townes.[1] The only way in which the mechanics of the molecular dissociation enters is via its influence on the Doppler line shape of the atomic fluorescence. The width of the emission is a critical parameter, however, since a larger width raises the threshold population required for maser oscillation and adds greatly to the difficulty of selecting a single mode.

We shall treat the dissociation of a diatomic gas by a beam of light by means of a simple semiclassical model. The main features derived from this will be seen to apply also to other dissociative processes and to polyatomic molecules.

although these will be considered only briefly here. The principal results are the distribution of velocity vectors of an atom A^* produced by

$$AB + h\nu_p \rightarrow (AB)^* \rightarrow A^* + B \qquad (1)$$

and the Doppler line shape of the atomic fluorescence,

$$A^* \rightarrow A + h\nu_F. \qquad (2)$$

In Section I we evaluate the "form factors" in the angular distribution of atoms, $I(\theta)$, and the Doppler line shape $D(\nu_F)$, which depend only on the orientation of the transition dipole moment within the molecule and the polarization of the pumping light. In Section II these factors are averaged over the thermal distributions of translational, rotational, and vibrational energy of the parent molecules, and the distribution of frequencies of the pumping light. The calculation of the form factors is entirely geometrical, whereas the averages over the energy distributions require knowledge of the potential curves of both the ground and excited electronic states of the AB molecule. In Section III we review experiments concerned with the anisotropy of the form factors, and discuss briefly some possible applications to optical masers.

I. GEOMETRICAL FACTORS IN PHOTODISSOCIATION

According to the Franck-Condon principle,[8] the position and momenta of the atomic nuclei remain constant during the electronic jump which accompanies the absorption of a photon. Ordinarily, if the excited electronic state subsequently dissociates, it does so in a time short compared with a rotational period of the molecule, and the distribution of trajectories of the fragment atoms reflects the initial orientation of the molecule. The photodissociating molecules are not isotropically distributed with respect to the exciting light beam, since the absorption probability is greatest when the transition dipole moment $\underset{\sim}{\mu}_{if}$ is aligned with the electric vector $\underset{\sim}{\mathcal{E}}$ of the light. Thus the angular distribution of the atoms should show a corresponding anisotropy.

The calculation of the form factors which characterize this anisotropy amounts to averaging the angular dependence of the transition probability, proportional to $|\underset{\sim}{\mu}_{if} \cdot \underset{\sim}{\mathcal{E}}|^2$, over all rotational orientations of the molecule. Several distinct cases appear. These are specified (see Table IV and Fig. 1) by the polarization of the exciting light; by the orientation of $\underset{\sim}{\mu}_{if}$, which is either parallel or perpendicular to the molecular axis; and by the direction of departure of the product atom, which is regarded as undergoing either axial recoil along the initial direction of the molecular axis, or

transverse recoil perpendicular to it. In Section II the general result will be synthesized from these two limiting cases for the recoil direction.

The orientation of the transition dipole moment,

$$\underset{\sim}{\mu}_{if} = \int \psi_i^* \, \underset{\sim}{\mu} \, \psi_f \, d\tau,$$

is readily identified from the symmetry properties of the initial and final molecular states.[9] As seen in Tables I and II, the allowed[10] $\Sigma \rightarrow \Sigma$, $\Pi \rightarrow \Pi$, and $\Delta \rightarrow \Delta$ transitions are parallel, and $\Sigma \rightarrow \Pi$ and $\Pi \rightarrow \Delta$ are perpendicular. The tables also include rules for electron impact recently derived by Dunn;[11] here the designation "parallel" or "perpendicular" refers to the orientation of the molecular axis with respect to a symmetry axis of the collision. For electron capture this symmetry axis lies along the incident electron beam. For dissociative excitation or ionization processes, a symmetry axis is less obvious, but can still be defined, as Dunn has shown. In many cases Dunn's rules predict anisotropies in the distribution of products which are qualitatively similar to those for photodissociation, and we shall make some comparisons in Section III.

The average over rotational orientations is conveniently formulated in terms of the Eulerian angles ϕ, θ, ψ which relate a rotating, "molecule-fixed" set of coordinate axes, xyz, to a nonrotating "space-fixed" system with axes parallel to specified laboratory directions, XYZ. For both systems the origin is the center-of-mass of atoms A and B. The angles

θ, ϕ are ordinary polar coordinates which locate the z-axis relative to the Z-axis and XY plane, and ψ is an azimuthal angle about the z-axis. Since all orientations of the molecule are equally likely,

$$\sin \theta \, d\theta \, d\phi \, d\psi \tag{3}$$

is the (unnormalized) probability of an orientation with Eulerian angles in the range θ, ϕ, ψ to $\theta + d\theta$, $\phi + d\phi$, $\psi + d\psi$. When the electric vector is aligned along one of the space fixed axes $F = X, Y, Z$, and the transition dipole moment lies along one of the molecule-fixed axes $g = x, y, z$, the absorption probability is proportional to

$$|\underset{\sim}{\mu} \cdot \underset{\sim}{\mathcal{E}}|^2 = \mu_g^2 \, \mathcal{E}_F^2 |\Phi_{Fg}(\phi, \theta, \psi)|^2, \tag{4}$$

since

$$\mu_F = \Sigma_g \, \Phi_{Fg} \, \mu_g \, .$$

(For simplicity we have dropped the subscripts from $\underset{\sim}{\mu}_{if}$.) Here the angle dependent factors Φ_{Fg} are the direction cosines which describe the orthogonal transformation[12] between the XYZ and xyz systems (see Table III). The probability that dissociation occurs for orientations in the range specified by (3) is thus given by

$$|\Phi_{Fg}(\phi, \theta, \psi)|^2 \sin \theta \, d\theta \, d\phi \, d\psi, \tag{5}$$

except for an angle independent normalization factor.

We shall choose the z-axis of the molecule-fixed system along the direction of departure of atom A, so that the polar

coordinates which describe the angular distribution become identical to the Eulerian angles θ and ϕ. For either axial or transverse recoil of A, we may obtain the intensity which enters the range θ, ϕ to $\theta + d\theta$, $\phi + d\phi$ by simply averaging (5) over ψ. By definition, this intensity is

$$I(\theta,\phi) \sin\theta \, d\theta \, d\phi ,$$

where $I(\theta,\phi)$ is the differential cross section per unit solid angle. Therefore we find

$$I_{Fg}(\theta,\phi) = \frac{1}{2\pi} \int_0^{2\pi} |\Phi_{Fg}(\phi,\theta,\psi)|^2 \, d\psi \qquad (6)$$

These functions are given in Table III.

As the transformation between the XYZ and xyz systems is orthogonal, the results for other cases of interest, in which $\underset{\sim}{\mu}$ or $\underset{\sim}{\mathcal{E}}$ have equal components along two axes, are obtained by merely summing terms of the appropriate form in (4), (5), and (6). To bring out the symmetry of the angular distributions, we chose the Z-axis along $\underset{\sim}{\mathcal{E}}$ in the case of plane polarized light, and along the direction of the beam for unpolarized light; thus we use the functions I_{Zg} or $I_{Xg} + I_{Yg}$, respectively, which are independent of ϕ. For axial recoil,

$$\mu_x = \mu_y = 0; \; \mu_z \neq 0 \text{ for } \parallel \text{ transitions},$$

$$\mu_x = \mu_y \neq 0; \; \mu_z = 0 \text{ for } \perp \text{ transitions},$$

since the molecular axis coincides with the z-axis. For transverse recoil, the molecular axis is taken along either the x or y axis and the μ_g components are permuted accordingly.

For example, in the case of unpolarized light, the angular distributions for the two types of electronic transitions are given by (except for normalization)

$$I_{||}(\theta) = I_{Xz} + I_{Yz}$$

and

$$I_{\perp}(\theta) = I_{Xx} + I_{Xy} + I_{Yx} + I_{Yy},$$

for axial recoil. The results for transverse recoil are obtained by $z \rightarrow x$ (or y), $x \rightarrow y$ (or z), $y \rightarrow z$ (or x). In Table IV formulas for the various cases are collected. These distributions have the form characteristic of a dipole interaction, $1 + aP_2(\theta)$, and satisfy the expected sum rules:[13]

$$\tfrac{1}{3}I_A(\theta) + \tfrac{2}{3}I_T(\theta) = 1 \qquad (7)$$

$$\tfrac{1}{3}I_{||}(\theta) + \tfrac{2}{3}I_{\perp}(\theta) = 1 . \qquad (8)$$

The angular distributions peak at right angles to the incident beam in those cases in which the direction of recoil coincides with the transition dipole moment (axial, parallel; or transverse, perpendicular); otherwise, the distributions peak forward and backward along the beam.

From Tables III and IV we may readily derive the corresponding form factors for the shape of the fluorescence line emitted by excited A^* atoms. At the low gas pressures of interest in maser experiments, the line shape is mainly determined by the Doppler effect, and other contributions will be

neglected. Since the relative displacement in frequency or wavelength is

$$(\nu - \nu_o)/\nu_o \cong (\lambda - \lambda_o)/\lambda_o = V_A/c, \qquad (9)$$

(where c denotes the speed of light), the Doppler line shape is proportional to the probability distribution of the component along the direction of observation of the velocity vector of atom A. The laboratory velocity is the resultant,

$$\underset{\sim}{V}_A = \underset{\sim}{C}_{AB} + \underset{\sim}{v}_A \qquad (10)$$

of the velocity of the center of mass of AB and the recoil velocity which carries A away from the center of mass. It is convenient, however, to derive first the geometrical form factors for $\underset{\sim}{C}_{AB} = 0$ and $\underset{\sim}{v}_A$ fixed in magnitude, and then construct from these the general result as shown in Section II.

These form factors for "recoil only" will be denoted by $R_F(v_F, v)$. They give the distributions of components v_F of the recoil velocity along the space-fixed axes when $\underset{\sim}{v}_A$ has the fixed magnitude v. The simplest method of evaluating the R_F functions permutes the axes so that the new set, X'Y'Z' has the Z'-axis along the direction of observation. The corresponding expressions for the angular distributions $I(\theta', \phi')$ are obtained as before from (6) and Table III. From the probability distribution for directions of $\underset{\sim}{v}_A$,

$$I(\theta', \phi') \sin \theta' \, d\theta' \, d\phi' ,$$

and the relation $v_F = v \cos \theta'$, we then obtain

$$R_F(v_F,v)dv_F = \frac{1}{2\pi}\int_0^{2\pi} I[\theta'(v_F,v),\phi']\,\frac{dv_F}{v}\,d\phi'. \qquad (11)$$

The integration (which eliminates all reference to the primed coordinate system) yields

$$R_F(v_F,v) = (1 + a_F P_{2F})R_o, \qquad (12)$$

with

$$\int_0^v R_F(v_F,v)dv_F = 1,$$

where R_o is the form factor for an isotropic distribution of recoil vectors,

$$R_o = 1/v, \text{ for } v \geq v_F \geq -v \qquad (13)$$

$$= 0, \text{ elsewhere}$$

and

$$P_{2F} = \frac{1}{2}\left(\frac{3v_F^2 - v^2}{v^2}\right). \qquad (14)$$

For observation along the Z-axis, the asymmetry parameter a_Z is the same as in Table IV, whereas for observation along the X or Y axes,

$$a_X = a_Y = -\frac{1}{2}\,a_Z\,. \qquad (15)$$

Thus, the average in (11) supresses part of the effect of the anisotropy in the angular distributions in the R_X and R_Y functions (which are identical) but not in the R_Z function. In Table V, the form factors are sorted into four classes, A

to D, characterized by decreasing anisotropy, and these are compared in Fig. 1. It is easily shown that the R_F functions satisfy sum rules analogous to (7) and (8), with unity replaced by R_o, and

$$\tfrac{1}{3}(R_X + R_Y + R_Z) = (1 + \tfrac{1}{2}a_Z P_{2Z})\, R_o \qquad (16)$$

Also, if the direction of observation does not coincide with one of the axes, but lies along a line L with polar angles Θ, Φ, the corresponding form factor is given by

$$R_L(v_L, v) = R_X \sin\Theta \cos\Phi + R_Y \sin\Theta \sin\Phi + R_Z \cos\Theta, \qquad (17)$$

where the arguments of the R_F functions are $v_X = v_L \sin\Theta \cos\Phi$, etc.

II. AVERAGES OVER ENERGY DISTRIBUTIONS

As indicated in (10), we must compound the form factors given in Table V with the distribution of center of mass velocity vectors and the distribution in magnitude of the recoil velocity. We shall denote by

$$D_F(V_F)dV_F,$$

the probability that atom A has a velocity component

$$V_F = C_F + v_F$$

in the laboratory-fixed coordinate system within the range V_F to $V_F + dV_F$. (For simplicity, the subscripts in (10) are henceforth omitted.) The Doppler line shape of the atomic fluorescence is obtained from $D_F(V_F)$ by replacing V_F with

$c(\nu-\nu_o/\nu_o)$. Since the distributions to be combined are independent, we have

$$D_F(V_F) = \int_0^{\infty} \int_{V_F-\nu}^{V_F+\nu} R_F(V_F-C_F,\nu)T(C_F)P(\nu)dC_F d\nu \qquad (18a)$$

or

$$= \int_0^{\infty} \int_{-\nu}^{\nu} R_F(v_F,\nu)T(V_F-v_F)P(\nu)dv_F d\nu \qquad (18b)$$

$T(C_F)$ is the translational velocity distribution,

$$T(C_F)dC_F = (1/\sqrt{\pi}\ \alpha)\exp(-C_F^2/\alpha^2)dC_F, \qquad (19)$$

where

$$\alpha = [2kT/(m_A+m_B)]^{1/2} \qquad (20)$$

is the most probable thermal velocity of an AB molecule. $P(\nu)$ is the recoil velocity distribution and is the only factor which depends on the detailed mechanics of photodissociation. In (18a), the line shape is constructed by regarding each point of the "recoil only" curve to be broadened by the translational distribution, whereas (18b) is the converse of this. The limits of integration are imposed by (13).

The average over the translational velocity distribution is conveniently formulated in terms of the error integral and its derivative,[14]

$$H(x) = (2/\sqrt{\pi}) \int_0^x e^{-z^2} dz; \quad H'(x) = (2/\sqrt{\pi})e^{-x^2},$$

and the dimensionless variables,

$$\xi = V_F/\alpha \; ; \quad \eta = v/\alpha \; .$$

Thus (18) yields

$$D_F(V_F) = \int_0^\infty F(\xi,\eta)[P(\alpha\eta)/\eta]d\eta \tag{21}$$

where

$$F(\xi,\eta) = \left[1+\tfrac{1}{2}(a_F/\eta^2)(3\xi^2-\eta^2+\tfrac{3}{2})\right]\left[H(\xi+\eta)-H(\xi-\eta)\right] \tag{22}$$

$$+\tfrac{3}{4}(a_F/\eta^2)\left[(\xi-\eta)H'(\xi+\eta)-(\xi+\eta)H'(\xi-\eta)\right]$$

As η ranges from small to large values, the $F(\xi,\eta)$ function varies between $T(\xi)$ and $R_F(\xi,\eta)$. For $\eta \gtrsim 1$, the line shape remains practically Gaussian, and therefore is not significantly affected by photodissociation. The half-width at half-intensity is closely approximated by the usual formula,[15]

$$\Delta\nu = (\nu_o/c)[(2kT/m)\ln 2]^{1/2}, \tag{23}$$

but with m the mass of the parent molecule rather than the atom. For $\eta \gtrsim 2$, the line shape is primarily determined by the "recoil only" form factor. This is illustrated in Fig. 2, which compares the $F(\xi,\eta)$ functions corresponding to the two most anisotropic cases of Table V.

The $P(v)$ distribution which governs the final average in (21) is determined by the shape of the potential curves for the ground and excited electronic states of the AB molecule, the thermal distributions of initial rotational and vibrational

energy, and the spectral distribution of the pumping light. In discussing these factors, we shall use the NaI molecule as an example.

According to an approximate form of the Franck-Condon principle,[16] the probability that an electronic jump to a repulsive potential curve V(r) takes place with the internuclear distance between r_o and $r_o + dr_o$ is proportional to

$$I_p \nu_p f_n |\psi_n(r_o)|^2 dr_o, \tag{24}$$

where ψ_n is the wavefunction for the nth vibrational level of the ground electronic state of AB, with energy E_n above the lowest level and relative population f_n; and the pumping light has intensity I_p at the frequency ν_p for which

$$V(r_o) = h\nu_p + E_n. \tag{25}$$

Fig. 3 shows the repulsive potential curve for the state of NaI which dissociates to form an excited Na(^{2}P) atom, as derived from these relations and fluorescence intensity measurements.[17] A portion of the potential curve for the ground electronic state is also shown, including the vibrational levels and their relative populations. The threshold energy $V(\infty) = 5.22 \pm 0.09$ ev is the sum of the NaI dissociation energy ($D_o = 3.12$ ev) recommended by Brewer[18] and the Na(^{2}P) excitation energy.

The final relative kinetic energy of the A^* and B atoms is

$$E = V(r_o) - V(\infty) + \tfrac{1}{2} (L^2/\mu r_o^2), \tag{26}$$

where μ is the reduced mass,

$$\mu = m_A m_B/m; \quad m = m_A + m_B,$$

and L is the initial rotational angular momentum of the excited $(AB)^*$ molecule, which is practically the same (except at low values of L) as the rotational momentum J of the ground state AB molecule. However, to obtain the appropriate statistical weight factors, f_L, we divide the relative populations of the rotational levels, f_J, by $(2J + 1)$, since the orientational degeneracy has already been accounted for in our calculation of the form factors. The recoil velocity $(v = v_A)$ of the A^* atom is given by

$$v_A(r_o, L) = (m_B/m)(2E/\mu)^{1/2}. \tag{27}$$

To evaluate the distribution function P(v), we have prepared a computer program which, for any specified potential functions, evaluates (27) for given values of r_o, n, and J, and compounds the weighting factors of (24) with f_L. Detailed calculations employing this program are described elsewhere.[19] For the present purpose, a simple approximation is sufficient. This considers only the population factors f_n and f_L and the most primitive form of the Franck-Condon Principle, which assumes that electronic jumps occur only from the midpoint when n = 0, and only from the turning points of the classical vibration when n > 0. Fig. 4 gives the P(v) functions derived in this way for various vibrational states of NaI; the subscripts

"L" and "H" for n > 0 distinguish the "low" and "high" jumps from the turning points.

We have considered axial and transverse recoil separately, in order to postpone the problem of treating the actual distribution of recoil directions. The trajectory of the A^* atom emitted in a photodissociation will approach an asymptotic line which makes an angle with the initial direction of the molecular axis. Axial recoil ($\chi = 0°$) is approached when

$$V(r_o) - V(\infty) >> L^2/2\mu r_o^2,$$

and transverse recoil ($\chi = 90°$) in the opposite limit. The angle of recoil is obtained by reversing the trajectory calculation for a two-body collision,[12] and this gives

$$\chi(r_o,L) = (L^2/2\mu)^{\frac{1}{2}} \int_{r_o}^{\infty} \left[V(r_o)-V(r) + \frac{L^2}{2\mu}\left(\frac{1}{r_o^2} - \frac{1}{r^2}\right)\right]^{-\frac{1}{2}} \frac{dr}{r^2} \quad (28)$$

The computer program[19] also evaluates (28) and the trajectories. Fig. 5 shows two sets of typical trajectories, one corresponding to the r_o at the midpoint of the n = 0 vibration, the other to the r_o for the "low" side of n = 4. As the latter transition is nearly at the threshold (see Fig. 3), the recoil angles become quite large. However, the statistical weight factor f_L favors low rotational energy and thus low values of χ, as is illustrated by the distributions given in Fig. 6.

To derive the angular distribution corresponding to a given value of χ, we return to (5) and introduce a new system of axes,

denoted by $g_r = x_r y_r z_r$ (with r for "recoil"), with the z_r axis parallel to the asymptote to the trajectory of A. The old "molecule-fixed" system, which we now denote by $g_m = x_m y_m z_m$, has z_m along the molecular axis. Thus χ is the polar angle relating the two systems; the g_r axes can be oriented so that the other two Eulerian angles vanish. The angles with respect to the "space-fixed" system, $F = XYZ$, are $\theta = \theta_r$, $\phi = \phi_r = \phi_m$, and $\psi = \psi_r = \psi_m$. The direction cosine elements $\Phi_{Fgm}(\phi, \theta_m, \psi)$ which appear in (4-6) are transformed into combinations of the $\Phi_{Fgr}(\phi, \theta, \psi)$ elements by an axis rotation, and thus

$$\Phi_{Fxm} = \Phi_{Fxr}$$

$$\Phi_{Fym} = \cos\chi\, \Phi_{Fyr} + \sin\chi\, \Phi_{Fzr}$$

$$\Phi_{Fzm} = -\sin\chi\, \Phi_{Fyr} + \cos\chi\, \Phi_{Fzr}$$

The calculation of the angular distribution now proceeds as before, and simply "mixes" the previous results for axial and transverse recoil,

$$I(\theta) = \cos^2\chi\, I_A(\theta) + \sin^2\chi\, I_T(\theta). \qquad (29a)$$

This may also be written as

$$I(\theta) = 1 + aP_2(\chi)P_2(\theta), \qquad (29b)$$

where a is the asymmetry parameter for the axial case given in Table IV. Analogous results obtain for the R_F form factors of Table V.

The average over the χ distribution can be readily incorporated in (21); in effect, we have $\chi = \chi(v)$, since (27) and (28) are determined by the same parameters and receive the same statistical weights. When $\chi = \chi_o$, with

$$\chi_o = \arccos(1/\sqrt{3}) = 54°44',$$

the angular distribution and the R_F factors correspond to isotropic recoil, as seen from (7). For $\chi < \chi_o$, the form factor for axial recoil gives the dominant contribution in (29). In the average the statistical factors usually strongly favor small values of χ, as illustrated in Fig. 6, and since $\cos^2\chi$ remains near unity in this region, the result is often practically equivalent to the case of purely axial recoil.

In Fig. 7 the combined effect of the various averages is illustrated for the most anisotropic form factor, Case A of Table V. The three uppermost curves refer to an $n = 3_L$ transition, and show R_F averaged over v (dot-dashed curve), over v and χ (dashed curve), and over v,χ, and the translational velocity distribution (solid curve). It is seen that even for this near threshold transition, which has a relatively broad distribution in χ (see Fig. 6), the line shape is quite close to that for purely axial recoil. The two lower curves refer to excitation by a rectangular band of pumping light with energy well above the threshold. Both curves have been averaged over v,χ, and translation; in one (dashed) the pumping band is narrow and excites only the $n = 0$ transition, in the other (solid) it is 500 Å wide and excites transitions from all the vibrational levels.

III. DISCUSSION

There have been many experimental studies of atomic fluorescence excited by molecular photodissociation, and a bibliography is given elsewhere.[19] In several cases, the presence of large Doppler broadening due to recoil has been established.[4,19] However, an early study of the NaI photodissociation by Mitchell appears to be the only attempt that has been made to observe a possible anisotropy in the angular distribution of products.[20] Mitchell viewed the fluorescent light through a sodium vapor filter, which transmitted only that part of the light for which the Doppler shift exceeded the absorption width of the filter. As he found no observable difference in the intensity of this filtered light emitted parallel and perpendicular to the incident beam, Mitchell concluded that the angular distribution of products was isotropic.[15,20]

This result is disappointing, but it is not incompatible with the treatment outlined here. The fluorescent Na(^{2}P) atoms could be formed by exciting either a $\Sigma \rightarrow \Sigma$ or a $\Sigma \rightarrow \Pi$ transition of NaI. According to Table V, since the exciting light was unpolarized the experiment involved a comparison of cases B and C, if the transition is $\Sigma \rightarrow \Sigma$, or cases C and D, if $\Sigma \rightarrow \Pi$. It is only necessary to consider the form factors of Fig. 1, as the recoil broadening is much larger than the thermal broadening (average $\eta \gtrsim 5$). Near the center of the fluorescence line, where sodium filter is most effective,

the ratio of the form factors is 2 for B/C and 0.7 for C/D, for axial recoil (the corresponding ratios are 0.7 and 1.2 for transverse recoil). Under the conditions of Mitchell's experiment, the filter removed up to 50% of the fluorescence intensity. Thus, the intensity observed parallel and perpendicular to the incident beam would be expected to change noticeably, by up to -25% for a $\Sigma \rightarrow \Sigma$ transition and up to +15% for $\Sigma \rightarrow \Pi$. However, if both these transitions were excited the anisotropy would be almost entirely suppressed, as an approximate sum rule analogous to (8) would apply. This explanation appears likely, since the bandwidth of the pumping light used by Mitchell was very broad, 0.3-0.5 ev, and there is some evidence[19] to suggest that the potential curves for the excited Σ and Π states differ by less than 0.3 ev over most of the relevant range of r_o.

Recently, the anisotropy of the photodissociation probability has been confirmed and explained in an elegant experiment on the H_2^+ molecular ion by Dehmelt and Jefferts.[21] This is not concerned with angular distributions of fluorescence but with the total photodissociation rates for the various spectroscopic states. The orientation dependence of these rates provides a means to accumulate molecules selectively in particular magnetic substates and to monitor the population changes induced by absorption of radiofrequency radiation. Dehmelt and Jefferts have derived in detail the photodissociation rates for the case of a parallel transition produced by polarized

light, and their analysis may readily be extended to the other cases considered in Table IV. The classical expressions for the rates are derived by averaging (5) over the molecular precessions characteristic of each spectroscopic state, and quantum mechanical results may be obtained by replacing the Φ_{Fg} factors of Table III with the well-known expressions for direction cosine matrix elements.[22]

Comparisons with molecular dissociation by electron impact are of particular interest, as maser pumping by electrons may sometimes be preferable to pumping by photons. The dissociative ionization of H_2 molecules by an electron beam has been found[23] to give an anisotropic distribution of protons, approximately of the form $1 + 2P_2(\theta)$, but there seems to be no experimental information about angular distributions for other systems. A theoretical calculation of the product distributions and fluorescence line shape would proceed just as for photodissociation, if the form factors of Tables IV and V were replaced by functions appropriate to electron impact. However, even in the Born approximation limit, the evaluation of the transition probability $P(\phi,\theta,\psi)$ which replaces $|\underset{\sim}{\mu} \cdot \underset{\sim}{\epsilon}|^2$ in (5) is a formidable numerical problem. Dunn's qualitative characterization of the anisotropies of $P(\phi,\theta,\psi)$ refers to two configurations in which the momentum transfer vector $\underset{\sim}{K}$ is aligned either parallel or perpendicular to the molecular axis.[11] According to the symmetry analysis summarized in Tables I and II, in most transitions $P(\phi,\theta,\psi)$ vanishes for one or another of these configurations, and then the dissociation products

will peak parallel or perpendicular to $\underset{\sim}{K}$ (only axial recoil is considered). In the case of dissociative electron capture or attachment, $\underset{\sim}{K}$ is identical to the propogation vector $\underset{\sim}{k}$ of the electron beam. For dissociative excitation or ionization, $\underset{\sim}{K}$ will have a range of orientations relative to $\underset{\sim}{k}$ (and described by an angle κ), and the factors involved in estimating this are also discussed by Dunn.

The peaking of the $P(\phi,\theta,\psi)$ functions with respect to $\underset{\sim}{K}$ may be expected to resemble qualitatively the peaking with respect to the electric vector which appears in photodissociation. Thus it is useful to note the connections given in Table VI, which obtain when $\underset{\sim}{K}$ is parallel ($\kappa = 0°$) or perpendicular ($\kappa = 90°$) to $\underset{\sim}{k}$. These connections become quantitative relations at sufficiently high energies, where the transition probability can be expanded with $|\underset{\sim}{\mu} \cdot \underset{\sim}{K}|^2$ as the leading term.[11] Again there appear two classes of electronic transitions, now classified as $\Delta\Lambda = 0$ ($\Sigma \rightarrow \Sigma$, $\Pi \rightarrow \Pi$, $\Delta \rightarrow \Delta$) and $\Delta\Lambda \neq 0$ ($\Sigma \rightarrow \Pi$, $\Sigma \rightarrow \Delta$, $\Pi \rightarrow \Delta$).

From Table VI we see that the case of dissociative electron capture (for which $\kappa = 0°$ always) is essentially equivalent to photodissociation with polarized light, except that some additional transitions become allowed. For dissociative electron excitation or ionization, we may expect to obtain a practical approximation to the general result by taking

$$I(\theta) = \cos^2\kappa I_c(\theta) + \sin^2\kappa I_s(\theta) \qquad (30)$$

and analogous expressions for the fluorescence form factors. (These mixing formulas are readily justified when the $|\mu \cdot K|^2$ term dominates the transition probability.) Here $I_c(\theta)$ denotes the result which applies for electron capture or polarized photodissociation, as given in the upper part of Table VI. In (30) this is reached in the limit of large momentum transfer (where $\underset{\sim}{k} \simeq \underset{\sim}{K}$ and hence $\varkappa \simeq 0°$), which obtains near the excitation or ionization threshold. We denote by $I_s(\theta)$ the result for small momentum transfer (where $\underset{\sim}{k} >> \underset{\sim}{K}$) and the conservation laws require $\varkappa \simeq 90°$), which obtains at high energy. This limit resembles closely photodissociation by unpolarized light, and is given in the lower part of Table VI. According to (30) and Fig. 1, in dissociative excitation the anisotropy in the form factors for a given transition will be a maximum at threshold, but will be first suppressed and then reversed in sense if the bombarding electron energy is increased sufficiently. In contrast, for dissociative capture the form factors should remain practically independent of the energy. The dissociation of polyatomic molecules by photons or electrons should also show anisotropies, since in many cases, the excitation probability will depend on the relative orientation of the incident beam and a molecular axis.[9,11]

In discussing the feasibility of optical masers utilizing excited atoms generated by molecular photodissociation, Singer and Gorog[5-7] have emphasized the importance of minimizing the fluorescence line width. As illustrated in our calculations, the width is quite sensitive to molecular properties, and in

particular to the shape of the potential curves. The width must therefore be investigated experimentally in each case. However, some general aspects of the problem are indicated by these calculations and the available data.[19]

The Doppler broadening arising from the thermal center-of-mass motion is somewhat less than that of an atom at the same temperature, as noted in (23). It can be almost eliminated by viewing the fluorescence at right angles to a molecular beam.[6,7] In practice, however, it appears that the dominant contribution to the Doppler width will usually come from the recoil velocity. An obvious way to minimize this is to use pumping light with energy only slightly above the threshold for producing fluorescence, so that $V(r_o)-V(\infty)$ in (26) is small. This approach usually involves a very substantial sacrifice in intensity as it discards molecules in the lowest vibrational states, which almost always lie under a strongly sloping portion of $V(r)$, as in Fig. 3. Also, even at the threshold, the thermal distribution of rotational energy still appears in the recoil velocity. Another means of limiting the recoil velocity is to select a molecule for which the mass factor in (27),

$$\left(\frac{m_B}{m_A m}\right)^{1/2},$$

is small. Unfortunately, other requirements often conflict with this. Finally, if the angular distribution is markedly

anisotropic, there is some advantage in observing the fluorescence at right angles to the preferred direction of recoil. For a "Case A" dissociation, the effective Doppler width is that of just one of the lobes. For the example of Fig. 7, we find $\Delta\nu = 3.6$, and 2.5, for $n = 0$, 3_L(solid), and 3_L(dashed), respectively.[24] From (23), the thermal center-if-mass motion alone would give $\Delta\nu = 2.5$, whereas for a Na atom at the same temperature $\Delta\nu = 6.3$. Thus, in this example it turns out that pumping at the $n = o$ transition would yield a fluorescence line half as wide (as well as four times more intense) as the line given by pumping at the $n = 3_L$ transition. The advantage which the $n = 3_L$ transition gains by being nearer to the threshold is overbalanced by the contributions from thermal motion and transverse recoil, which blur together the two lobes of the fluorescence line. The "recoil splitting" and consequent narrowing of the fluorescence line predicted for Case A would be destroyed if $\Sigma \rightarrow \Sigma$ and $\Sigma \rightarrow \Pi$ transitions are superimposed as seems likely for NaI. The $\Delta\nu$ for the $n = 0$ transition in Fig. 7 becomes 10 for a Case B dissociation, and 15 for isotropic recoil.

Table I. Behavior of the transition probability between pairs of electronic states of homonuclear diatomic molecules. Behavior for parallel transitions is indicated to the right of the vertical line, for perpendicular transitions to the left. The transition probability for electric dipole transitions induced by photons is nonvanishing only where a P appears; the transition probability for "aligned" collisions (see text) with electrons is nonvanishing where either a P or an E appears.

	Σ_g^+	Σ_g^-	Σ_u^+	Σ_u^-	Π_g	Π_u	Δ_g	Δ_u
Σ_g^+	E|E	0|0	0|P	0|0	0|0	P|0	E|0	0|0
Σ_g^-		E|E	0|0	0|P	0|0	P|0	E|0	0|0
Σ_u^+			E|E	0|0	P|0	0|0	0|0	E|0
Σ_u^-				E|E	P|0	0|0	0|0	E|0
Π_g					E|E	0|P	0|0	P|0
Π_u						E|E	P|0	0|0
Δ_g							E|E	0|P
Δ_u								E|E

Table II. Behavior of the transition probability between pairs of electronic states of heteronuclear diatomic molecules. Notation is the same as in Table I.

	Σ^+	Σ^-	Π	Δ
Σ^+	E|P	0|0	P|0	E|0
Σ^-		E|P	P|0	E|0
Π			E|P	P|0
Δ				E|P

Table III. Transformation coefficients in terms of Eulerian angles.

Direction of Transition Dipole	Direction of Electric Field F=X	Y	Z
	Direction cosine factors, Φ_{Fg}		
g=x	$C\phi C\psi - S\phi C\theta C\psi$	$S\phi C\psi + C\phi C\theta S\psi$	$S\theta S\psi$
y	$-C\phi S\psi - S\phi C\theta C\psi$	$-S\phi S\psi + C\phi C\theta C\psi$	$S\theta C\psi$
z	$S\phi S\theta$	$-C\phi S\theta$	$C\theta$
	Azimuthally averaged squares, $\frac{1}{2\pi}\lvert\Phi_{Fg}\rvert^2$		
x or y	$\frac{1}{2}(C_\phi^2 + S_\phi^2 C_\theta^2)$	$\frac{1}{2}(S_\phi^2 + C_\phi^2 C_\theta^2)$	$\frac{1}{2}S_\theta^2$
z	$S_\phi^2 S_\theta^2$	$C_\phi^2 S_\theta^2$	C_θ^2

Here sine is abbreviated by S, cosine by C.

Table IV. Differential cross section $I(\theta)$ in center-of-mass system.

Electronic Transition	Axial Recoil	Transverse Recoil
For polarized light with electric field along Z-axis		
$\parallel$	$1 + 2P_2$	$1 - P_2$
$\perp$	$1 - P_2$	$1 + \frac{1}{2}P_2$
For unpolarized light incident along Z-axis		
$\parallel$	$1 - P_2$	$1 + \frac{1}{2}P_2$
$\perp$	$1 + \frac{1}{2}P_2$	$1 - \frac{1}{4}P_2$

where

$$P_2 = \frac{1}{2}\left(3\cos^2\theta - 1\right)$$

$$\int_0^{2\pi}\int_0^{\pi} I(\theta)\sin\theta\, d\theta\, d\phi = 4\pi$$

Table V. Form factors R_F for recoil broadening of atomic fluorescence line.

Electronic Transition	Light Beam	Observation Direction	Axial Recoil	Transverse Recoil
Case A				
$\parallel$	p	Z	$1 + 2P_{2F}$	$1 - P_{2F}$
Case B				
$\perp$	p	Z		
$\parallel$	u	Z	$1 - P_{2F}$	$1 + \frac{1}{2}P_{2F}$
$\parallel$	p	X or Y		
Case C				
$\perp$	u	Z		
$\parallel$	u	X or Y	$1 + \frac{1}{2}P_{2F}$	$1 - \frac{1}{4}P_{2F}$
$\perp$	p	X or Y		
Case D				
$\perp$	u	X or Y	$1 - \frac{1}{4}P_{2F}$	$1 + \frac{1}{8}P_{2F}$

Here p denotes polarized light with the electric vector along the Z-axis and u unpolarized light incident along the Z-axis. These formulas are to be multiplied by the isotropic factor R_o as in equation (12).

Table VI. Comparison of dissociative electron impact with photodissociation.

Electronic Transition	Angular Distribution	Fluroescence Z	Fluroescence X or Y
Momentum transfer along beam ($\kappa=0°$)			
$\Delta\Lambda = 0$	A	A	B
$\Delta\Lambda \neq 0$	B	B	C
Momentum transfer transverse to beam ($\kappa=90°$)			
$\Delta\Lambda = 0$	B	B	C
$\Delta\Lambda \neq 0$	C	C	D

Here A to D designate form factors which are expected to resemble qualitatively those given for axial recoil in Table V and Fig. 1. The electron beam is incident along the Z-axis.

Captions for Figures

Fig. 1—Form factors, $1 + aP_2$, for axial recoil (solid curves) and transverse recoil (dashed curves), for the various cases defined in Table V. Cases A, B, C apply also to the differential cross sections of Table IV.

Fig. 2—Line shape functions $F(\xi,\eta)$ versus ξ for various values of a, the asymmetry parameter of Table V, and η, the ratio of the recoil velocity and the most probable translational velocity.

Fig. 3—Potential curves for the NaI molecule (after Hansen[17]).

Fig. 4—Distribution of recoil velocity of Na atoms produced by photodissociation of NaI molecules in various vibrational levels. The sloping curves which extend to higher velocities arise from the rotational contribution in equation (26).

Fig. 5—Trajectories of Na atoms produced by photodissociation of NaI molecules in various vibrational states, n, and rotational states, J. The distance between the recoiling Na and I atoms exceeds 100 Å within less than 10^{-13} seconds, for n = 0, and less than 5×10^{-11} seconds, for $n = 4_L$.

Fig. 6—Distributions of recoil angles. These correspond to the velocity distributions of Fig. 4.

Fig. 7—Doppler line shapes calculated for fluorescence of Na atoms produced in a Case A transition of NaI (see Table V). The area under the $n = 3_L$ curves should be reduced by one-third when comparisons with the other curves are made. A velocity of 10^5 cm/sec corresponds to a Doppler shift of 0.020 Å.

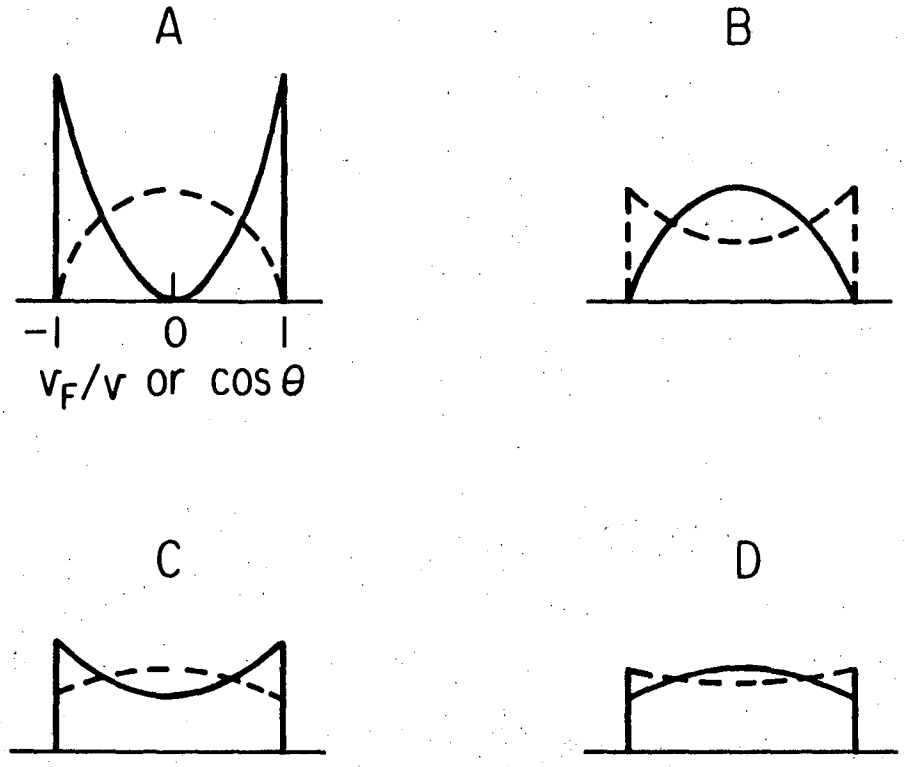

Fig. 1.

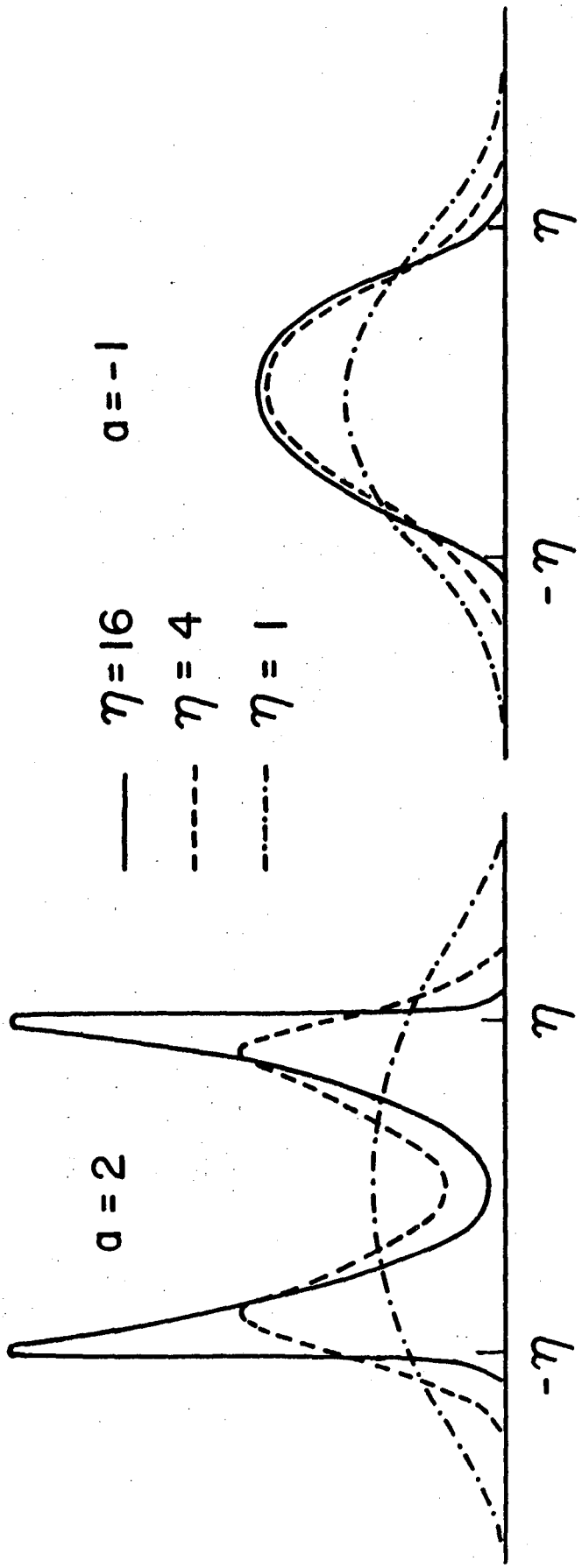

Fig. 2.

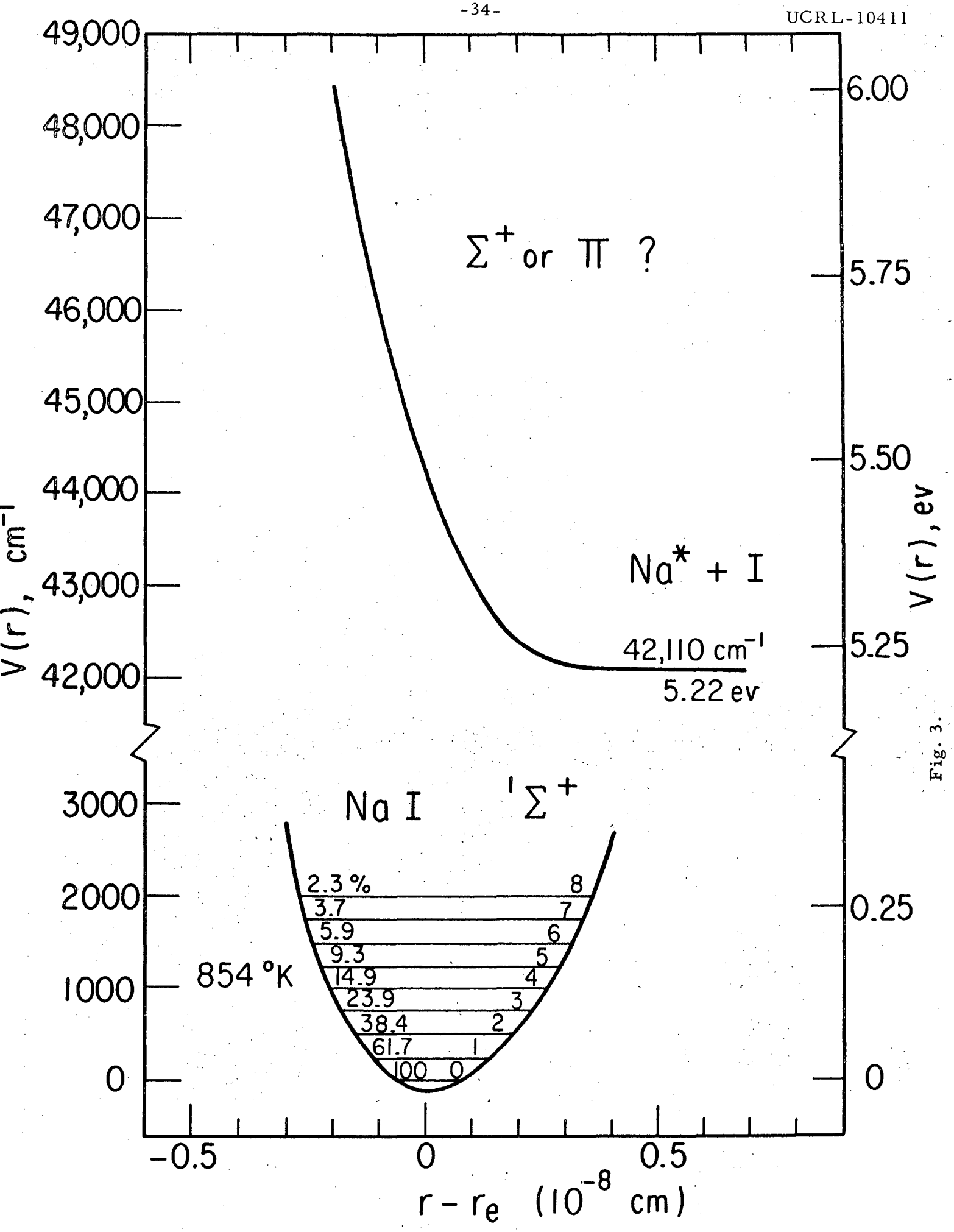
49,000
48,000
47,000
46,000
45,000
44,000
43,000
42,000
3000
2000
1000
0
V(r), cm⁻¹
6.00
5.75
5.50
5.25
0.25
0
V(r), ev
Σ⁺ or Π ?
Na* + I
42,110 cm⁻¹
5.22 ev
Na I ¹Σ⁺
854 °K
2.3 %
3.7
5.9
9.3
14.9
23.9
38.4
61.7
100
8
7
6
5
4
3
2
1
0
-0.5
0
0.5
r - re (10⁻⁸ cm)

Fig. 3.

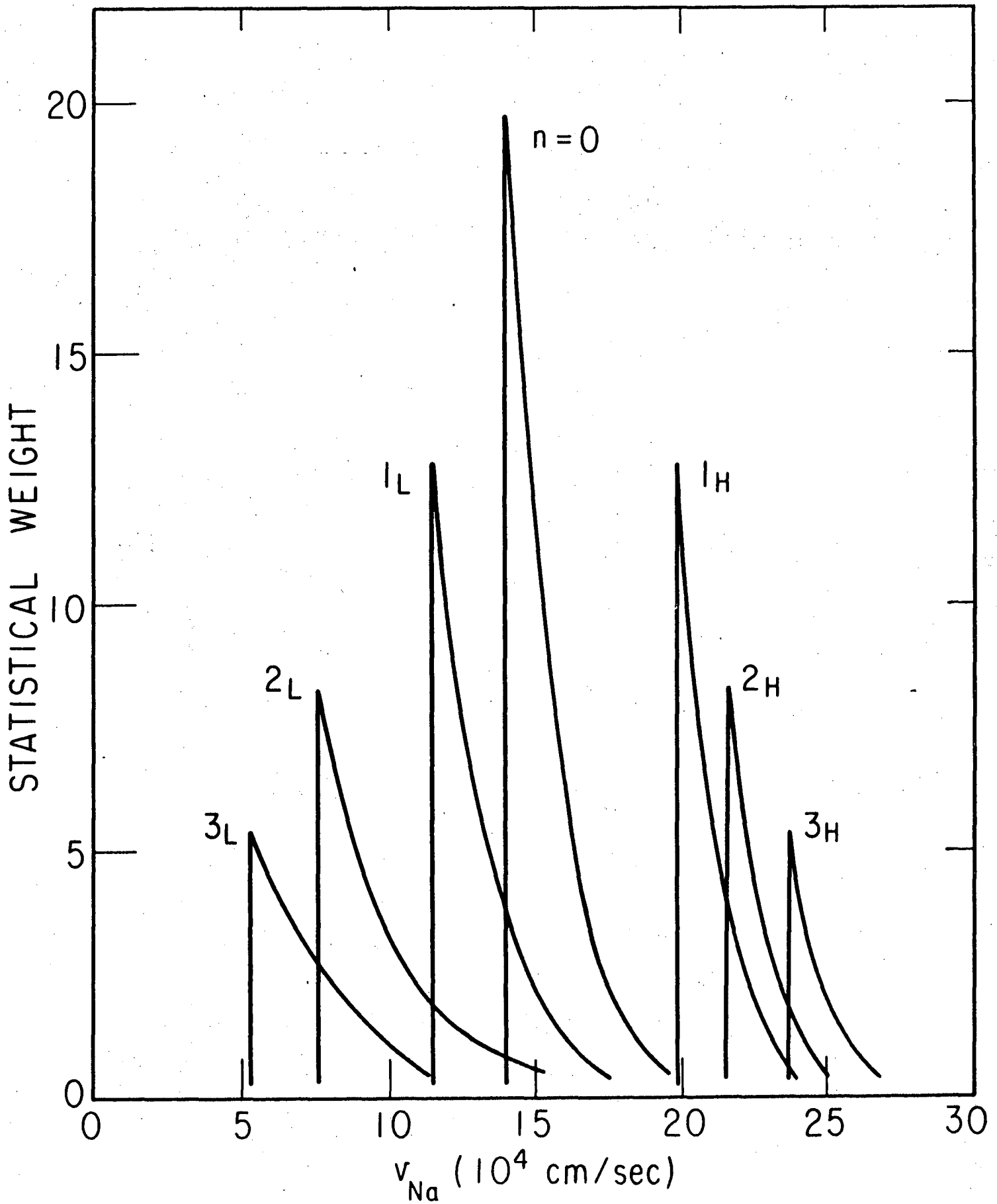
n = 0
1L
1H
2L
2H
3L
3H
STATISTICAL WEIGHT
0
5
10
15
20
0
5
10
15
20
25
30
v_{Na} (10^4 cm/sec)

Fig. 4.

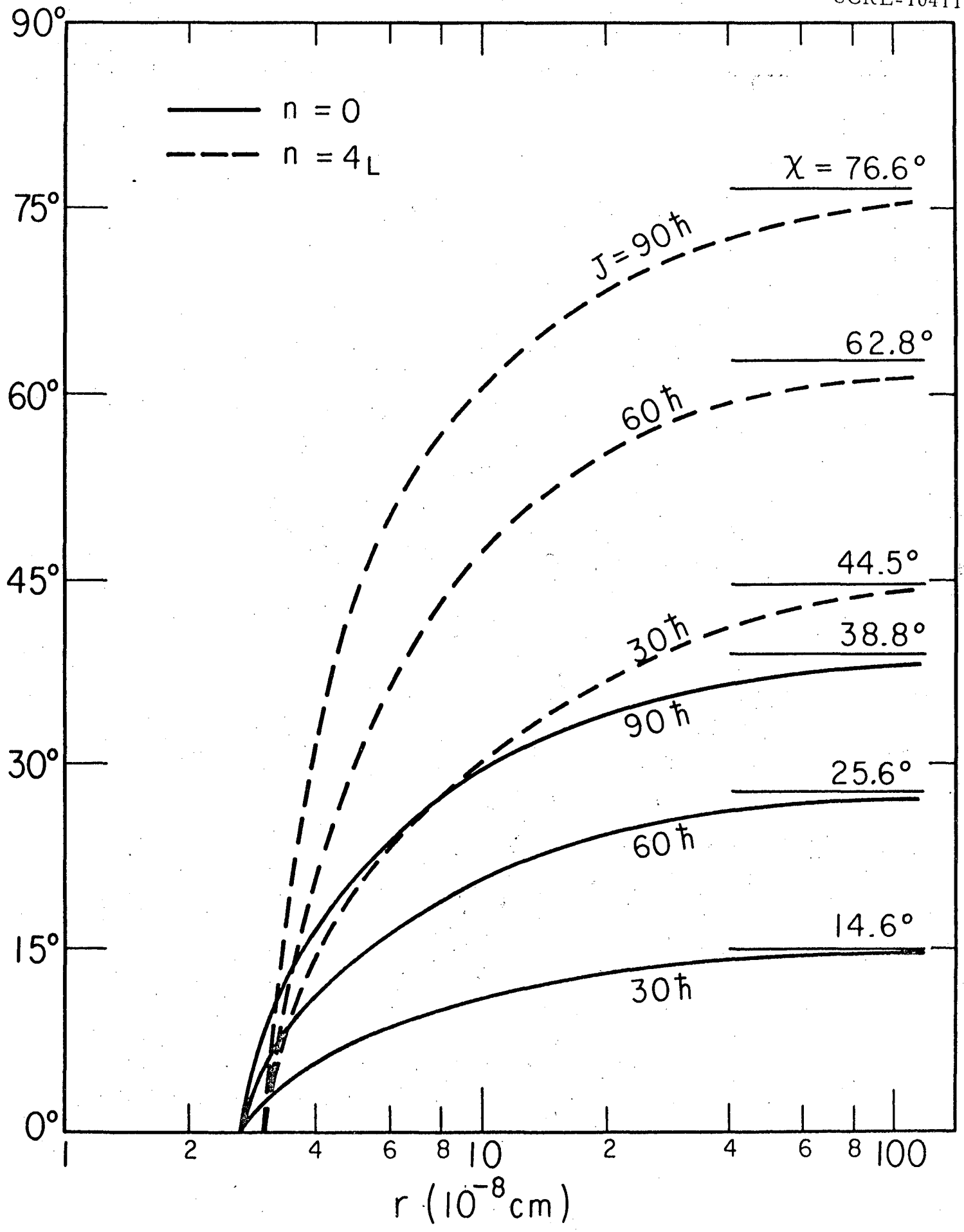
90°
75°
60°
45°
30°
15°
0°
n = 0
n = 4L
χ = 76.6°
J=90ħ
62.8°
60ħ
44.5°
30ħ
38.8°
90 ħ
25.6°
60 ħ
14.6°
30ħ
1
2
4
6
8
10
2
4
6
8
100
r (10⁻⁸cm)

Fig. 5.

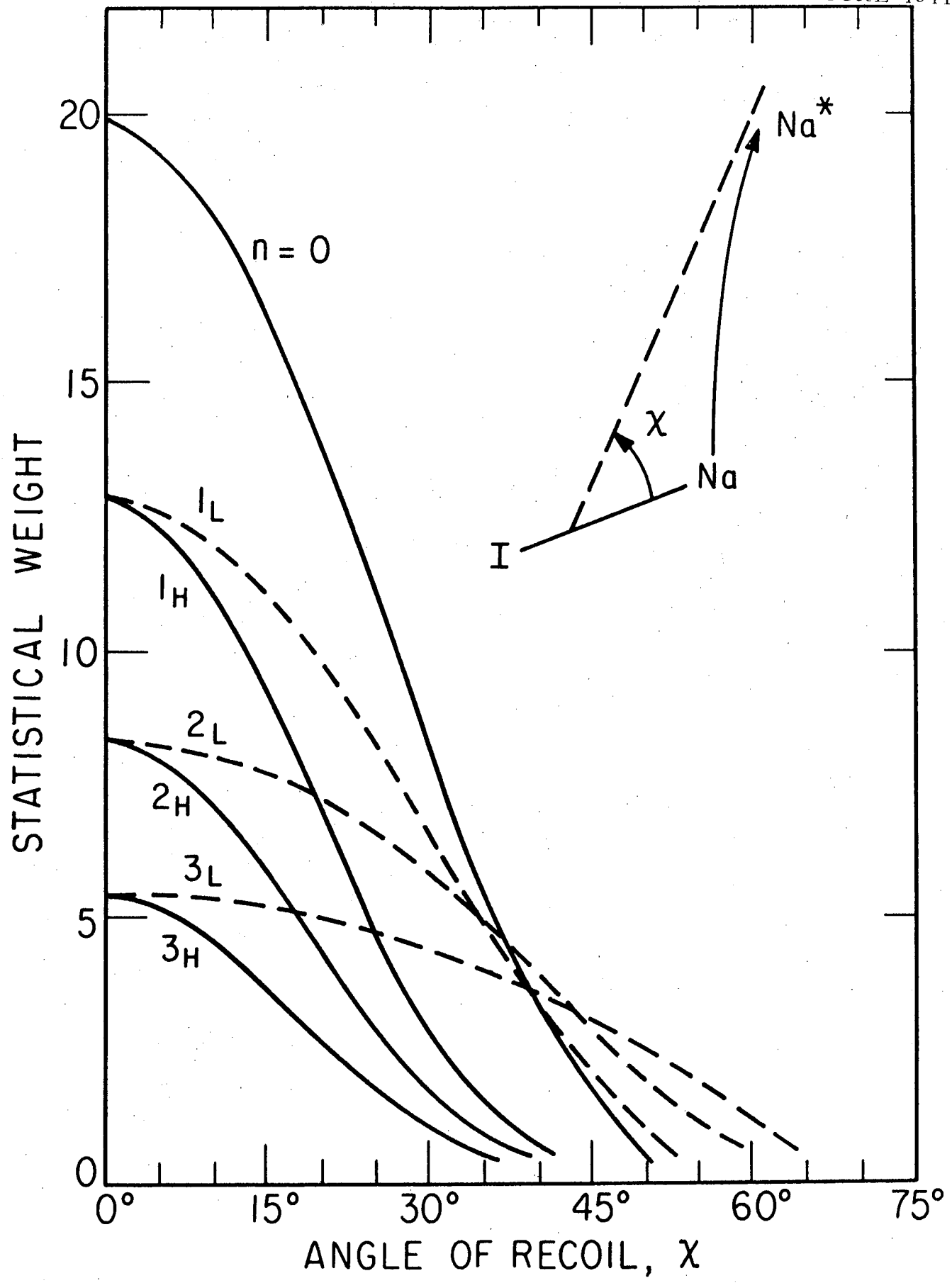
STATISTICAL WEIGHT
20
15
10
5
0
n = 0
1_L
1_H
2_L
2_H
3_L
3_H
Na*
χ
Na
I
0°
15°
30°
45°
60°
75°
ANGLE OF RECOIL, χ

Fig. 6.

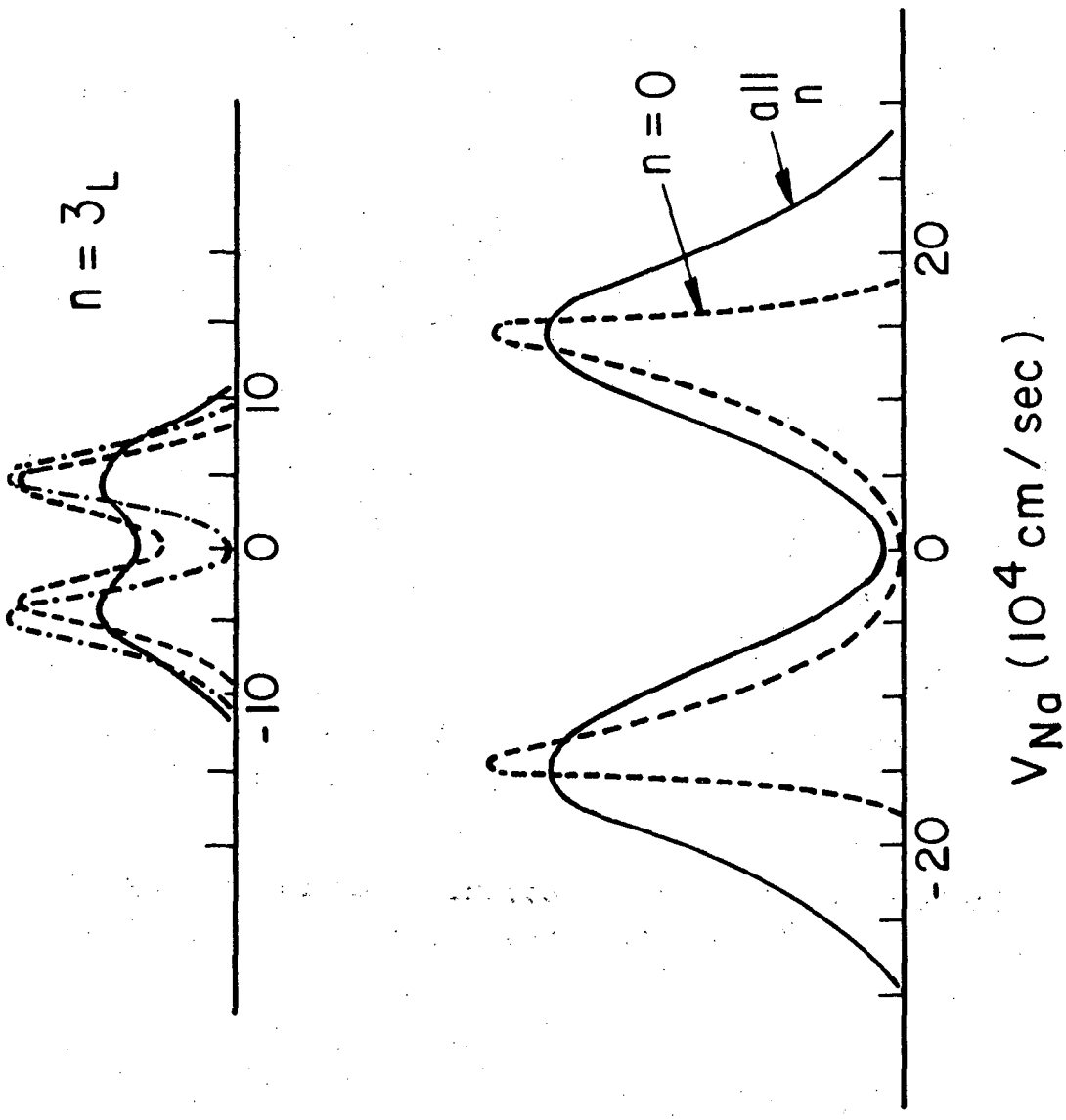

Fig. 7.

Footnotes

1. A. L. Schawlow and C. H. Townes, "Infrared and Optical Masers," Phys. Rev., Vol. 112, pp. 1940-1949; December, 1958.

2. C. H. Townes, Ed., "Quantum Electronics," Columbia University Press, New York, N.Y.; 1960.

3. J. R. Singer, Ed., "Advances in Quantum Electronics," Columbia University Press, New York, N.Y.; 1961.

4. P. Pringsheim, "Fluorescence and Phosphorescence," p. 208, Interscience Publishers, Inc., New York; 1949.

5. J. R. Singer, "Masers and Other Quantum Mechanical Amplifiers," Advances in Electronics and Electron Physics, Vol. 15, pp. 73-162, Academic Press, New York, N.Y.; 1961.

6. J. R. Singer and I. Gorog, "Optical Masers Utilizing Molecular Beams," Bull. Am. Phys. Soc. p. 14, January, 1962.

7. I. Gorog, "Coherent Optical Emission from Molecular Beams," Electronics Research Laboratory (M.S. Thesis) University of California, Berkeley, California; November, 1961.

8. E. U. Condon, "The Franck-Condon Principle and Related Topics," Am. Journal of Phys. Vol. 15, pp. 365-374; September, 1947.

9. H. Sponer and E. Teller, "Electronic Spectra of Polyatomic Molecules," Rev. Mod. Phys. Vol. 13, pp. 75-169; April, 1941.

10. The Selection rules given in Tables I and II disregard electronic-rotational coupling.

11. G. H. Dunn, "Anisotropies in Angular Distributions of Molecular Dissociation Products," Phys. Rev. Letters, Vol. 8, pp. 62-64; January, 1962.

12. H. Goldstein, "Classical Mechanics," Addison-Wesley Publishing Company, Inc., Reading, Mass.; 1957.

13. Indeed, from relations (7) and (8), one can infer the relative signs and magnitudes of the asymmetry parameter a, for the various cases of Table IV, but not the absolute magnitude.

14. An extensive tabulation of these functions is given in "Tables of Probability Functions," Vol. I, National Bureau of Standards, Washington, D.C.; 1941.

15. A. C. G. Mitchell and M. W. Zemansky, "Resonance Radiation and Excited Atoms," Cambridge University Press; 1961.

16. G. Herzberg, "Spectra of Diatomic Molecules," p. 393, D. Van Nostrand Company, Inc. Princeton, N.J., 1961.

17. H. G. Hanson, "Quenching of NaI Fluorescence by H_2, HCl, CO_2 and H_2O," Journal of Chem. Phys. Vol 23, pp. 1391-1397; August, 1955.

18. L. Brewer and E. Brackett, "The Dissociation Energies of Gaseous Alkali Halides," Chem. Rev. Vol. 61, pp. 425-432; August, 1961.

19. R. N. Zare and D. R. Herschbach, "Mechanics of Molecular Photodissociation," UCRL Report 10438, Lawrence Radiation Laboratory, University of California, Berkeley; September 1962.

20. A. C. G. Mitchell, "Über die Richtungsverteilung der Relativgeschwindigkeit der Zerfallsprodukte bei der optischen Dissoziation von NaJ," Zeit. f. Physik, Vol. 49, pp. 228-235; 1928.

21. K. B. Jefferts and H. G. Dehmelt, "Experimental Demonstration of Alignment of H_2^+ Molecular Ions by Selective Photodissociation," Bull. Am. Phys. Soc. Vol. 7, p. 432; August, 1962. See also; H. G. Dehmelt and K. B. Jefferts, "Alignment of the H_2^+ Molecular Ion by Selective Photodissociation. I," Phys. Rev. Vol. 125; pp. 1318-1322; February, 1962.

22. See, for example, P. C. Cross, R. M. Hainer and G. W. King, "The Asymmetric Rotor II. Calculation of Dipole Intensities and Line Classification," Journal of Chem. Phys. Vol. 12, pp. 210-243; June, 1944.

23. V. N. Sasaki and T. Nakao, "Molekulare Orientierung ung die Anregungs-und Die Anregungs - und Wasserstoff-moleküls durch Elektronenstoss," Proc. Imp. Acad. Japan, Vol. 11, pp. 413-415; December, 1935. See also, V. N. Sasaki and T. Nakao, "Molekulare Orientierung und die Dissoziationswahrscheinlichkeit des Wasserstoffmoleküls durch Electronenstoss," Proc. Imp. Acad. Japan, Vol. 17, pp. 75-77; March, 1941.

24. For convenience, we omit the factor ν_o/c and give $\Delta\nu$ in velocity units, 10^4 cm/sec.